



ELSEVIER

Available online at www.sciencedirect.com

SCIENCE @ DIRECT®

Nuclear Physics A 752 (2005) 679c–687c

NUCLEAR
PHYSICS **A**

Positron Emission Tomography: Principles, Technology, and Recent Developments

Sibylle I. Ziegler

Nuklearmedizinische Klinik, Klinikum rechts der Isar der Technischen Universität München, Ismaninger Str. 22 D-81675 München, Germany

Positron emission tomography (PET) is a nuclear medical imaging technique for quantitative measurement of physiologic parameters *in vivo* (an overview of principles and applications can be found in [1]), based on the detection of small amounts of positron-emitter-labelled biologic molecules. Various radiotracers are available for neurological, cardiological, and oncological applications in the clinic and in research protocols. This overview describes the basic principles, technology, and recent developments in PET, followed by a section on the development of a tomograph with avalanche photodiodes dedicated for small animal imaging as an example of efforts in the domain of high resolution tomographs.

1. PRINCIPLES OF POSITRON EMISSION TOMOGRAPHY

PET is based on the detection of very small (picomolar) quantities of biological substances which are labelled with a positron emitter. Most commonly used are carbon-11, oxygen-15, nitrogen-13, and fluorine-18. Advantages of positron labelled substances are their very high specificity (molecular targeting), the possibility of using biological active substances without changing their behaviour by the label, and fulfilment of the tracer principle. Thus, the process of interest remains unchanged during the measurement. Target structures of these molecules are e.g. glucose metabolism, receptor binding potential, catecholamine transport, amino acid transport, or protein synthesis. All the above mentioned nuclides have very short radioactive half-lives (2 min for O-15, 109 min for F-18), which necessitates a nearby cyclotron and radiochemistry facility.

Imaging of regional tracer concentration is accomplished by the unique properties of positron decay and annihilation. After the emission from the parent nucleus, the energetic positron traverses a few millimeters through the tissue until it becomes thermalized by electrostatic interaction between the electrons and the atomic nuclei of the media and combines with a free electron to form a positronium. The positronium decays by annihilation, generating a pair of gamma rays which travel in nearly opposite directions with an energy of 511 keV each. The opposed photons from positron decay can

be detected by using pairs of collinearly aligned detectors in coincidence. This “electronic collimation” is the reason why PET is much more sensitive (factor >100) than the conventional nuclear medical technique, namely single photon emission tomography (SPECT) using gamma cameras and lead collimators. The detector pairs of a PET system are installed in a ring-like pattern, which allows measurement of radioactivity along lines through the organ of interest at a large number of angles and radial distances. Subsequently, this angular information is used in the reconstruction of tomographic images of regional radioactivity distribution. State-of-the-art positron emission tomographs consist of multiple, closely packed rings of detectors that enable simultaneous imaging of several image planes. Coincident events between rings of the camera are acquired to generate cross-data, which minimizes data gaps between imaging planes. Such data acquisition allows almost complete data sampling in three dimensions (3D PET). The raw data are integrals along the line-of-coincidence over the activity distribution. There is no time-of-flight information included since the timing resolution of the current detectors is not good enough.

Reconstruction algorithms are used to calculate the underlying activity distribution. Statistical, iterative reconstruction algorithms have become the method of choice in many cases because of their superior image quality compared to traditional filtered backprojection methods. Briefly, their basic principle is as follows. Starting from an initial guess for the activity distribution, data are forward projected according to the scanner geometry, the resulting projections are compared to the measured projections and the error-projection is used for correcting the estimate. The new estimate is then forward projected and the comparison between estimated and measured projections yields the next correction. This loop is iterated until estimated and measured projections agree within their statistics. Improved availability of computing power and the introduction of fast algorithms [2-4] have introduced these methods in routine use.

The spatial resolution which can be achieved in a PET image is principally limited by positron range and gamma ray non-collinearity. In addition, the width of the detection elements in the tomograph determines the width of the coincidence response function and thus the image resolution.

2. PET TECHNOLOGY

A state-of-the art PET system has an axial field-of-view of about 18 cm and acquires coincidence data in the so-called 3D-mode, accepting data along even very oblique angles. The sketch in figure 1 shows the possible event types in 3D PET.

While the sensitivity of 3D PET is obviously high, the amount of scattered radiation which is measured is significant (it can be more than 50% of the total measured counts in a standard whole-body scan). For improved 3D acquisition characteristics, requirements for the detector systems are:

High Z material. Interaction probability and photo fraction for 511 keV should be high so that gamma rays are efficiently detected and chances for multiple interactions in finely granulated detector elements are minimized.

Good energy resolution. For 3D PET it is essential to reduce the fraction of detected scattered gamma rays as much as possible.

Short coincidence window. Good timing is the prerequisite for random reduction.

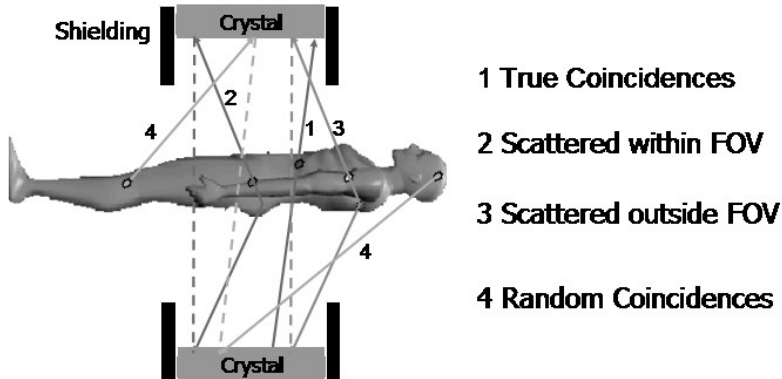


Fig. 1: PET event types. In addition to true events (1), scattered events (2,3) in which one or both of the detected gamma rays changed their original flight direction and random coincidences (4) are measured, resulting in a reduced signal to background ratio. Dashed lines indicate the line of response to which the events are falsely attributed.

Table 1 summarizes the most important characteristics of PET scintillation crystals, compared to the standard gamma camera scintillator, NaI.

Table 1: Characteristics of scintillation crystals for PET

	NaI	BGO	LSO	GSO
	NaI(Tl)	$\text{Bi}_4\text{Ge}_3\text{O}_{12}$	$\text{Lu}_2\text{SiO}_5:\text{Ce}$	$\text{Gd}_2\text{SiO}_5:\text{Ce}$
Density (g/cm^3)	3.7	7.1	7.4	6.7
Effective Z	51	75	65	59
Atten. length at 511 keV (mm)	29.1	10.4	11.4	14.1
Light yield (photons/MeV)	41000	9000	26000	8000
Decay time (ns)	230	300	40	60
Emission (nm)	410	480	420	440

BGO was basically the PET scintillator for a long time. Because of its long scintillation light decay time and therefore long coincidence timing windows of around 20 ns, and because of its low energy resolution, it almost exclusively was used in the 2D-

mode with thin absorbing septa in between the detector rings to reduce scatter. The fast, cerium doped oxy-orthosilicates, LSO and GSO (see table 1), are now used in commercial PET scanners for improved 3D performance.

As stated above, the size of the scintillation crystal determines the intrinsic spatial resolution of the tomograph. Readout schemes are used to couple a large number of small crystal elements onto photomultiplier tubes with larger area. The commonly used principle is the block detector. This concept uses light sharing and centroid calculation in four photomultiplier tubes to identify in which crystal of an e.g. 8x8 crystal matrix the gamma ray was detected [5]. Another approach is the use of a continuous light guide coupling small crystal elements to an array of photomultiplier tubes [6, 7]. The spatial resolution which can be achieved with clinical tomographs is 4-6 mm (FWHM) and the axial field-of-view ranges from 15 to 18 cm [8-11].

2. QUANTIFICATION

In order to achieve quantitative information, corrections for dead time, randoms, scatter and attenuation need to be performed. Random coincidences are usually subtracted by the delayed coincidence method, while scatter subtraction is based on model calculation. Correction of photon attenuation is the by far largest correction. Since both annihilation photons are measured, the factor by which the count rate in any line-of-response is reduced, is the same as for an external source along that line. External rotating pin sources are used to perform a transmission scan which allows the measurement of regional attenuation factors.

Once the corrections have been applied and the scanner count rate has been calibrated versus true activity concentration, the pixel values in the image are in Bq/ml. Time sequences can be acquired (4D PET) which build the basis for compartmental modeling aiming at measuring physiological constants such as metabolic or transport rates.

3. APPLICATION OF PET

Most clinical PET studies are performed to determine the extent of a tumor and the location and number of metastases. Fluorine-18 labelled Fluorodeoxyglucose (FDG), a sugar analogue, is used for tumour detection and staging, using the fact that tumour cells have an increased glucose uptake compared to normal tissue. FDG is taken up by the cell in the same way as glucose but it is not further metabolized. This trapping effect is very useful for imaging purposes since a single scan at a given time after injection of the radiotracer will show activity concentrations which are proportional to FDG consumption. The most commonly employed PET protocol is the whole body scan: About 40 min after intravenous injection of approx. 400 MBq FDG the patient is positioned on the scanner bed and acquisitions of one to ten bed positions are performed. Total scanning time with modern LSO or GSO-based systems is around 30 min for a 10 bed positions whole body scan. Figure 2 shows an example of FDG uptake in a

patient with metastases from colon cancer. The increased glucose uptake in cancer tissue is easily visible.

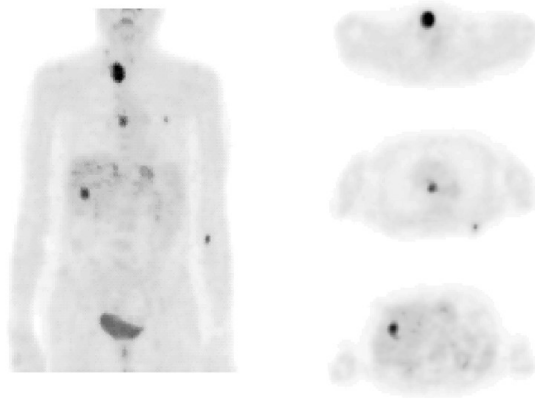


Fig. 2: Whole-body FDG study of a patient with metastases from colon cancer (left: projection, right: Three representative transaxial slices). Measurement started 40 min after injection of 370 MBq F-18 FDG.

Other clinical applications of FDG include brain scans for diagnosing Alzheimer's disease. Tumours in the brain are imaged using amino acids since the normal glucose uptake of the brain is very high, thus only little contrast can be achieved with FDG in cancer tissue.

Since PET tracers are very specific and very little anatomical information can be found in PET images, the joint reading of PET and CT or MR images is clinical routine. This was the impetus for the development of combined PET/CT tomographs (see e.g. [12, 13]). In these devices, a PET scanner and an x-ray CT are built in the same gantry, allowing the acquisition of PET as well as CT data with minimum time delay. The advantages are manifold: For example, coregistration of function (PET) and anatomy (CT) is straight forward and the CT data can be used for PET attenuation correction after appropriate scaling. Problems arise from the fact that CT is much faster (seconds) than PET (minutes) and effects from respiratory motion need to be minimized.

PET/CT has been widely accepted and it can be anticipated that these combined devices will be the standard in the near future. Further improvements in the direction of increasing PET sensitivity and exploiting the power of PET/CT for cardiac applications are underway.

4. NEW DEVELOPMENTS

New developments in the area of PET detectors are aimed at improving spatial resolution and sensitivity. Most recently, new, fast and luminous scintillators have been characterized. One example is LaBr_3 which may improve the signal-to-noise ratio in whole-body PET [14], or could even be used for time-of-flight PET.

Small animal imaging, which uses molecular imaging for the functional characterization of disease models in rats or mice, has triggered a wide range of efforts to improve PET performance. The field of animal PET is a very active research area with many approaches based on technology originating from nuclear physics. This involves new scintillation crystals, various ways of reading out an array of crystals with photo sensors, introduction of new photo sensors, or the use of scintillator-free detectors such as gas avalanche detectors (for an overview on animal PET see for example [15]).

Because for small ring diameters the parallax error becomes significant, methods for measuring the depth-of-interaction in the detector volume are investigated to improve spatial resolution in the whole field-of-view.

A system (MADPET-II) which is under development in our lab (Nuclear Medicine Clinic, Technische Universität München) addresses two new technologies in animal PET:

1. The use of avalanche photodiode arrays (APDs) to read out small, individual LSO crystals with a one-by-one scheme. In a prototype the feasibility of combining APDs and LSO for a research tomograph had been shown [16].
2. Two radial detector layers for depth-of-interaction measurement. Each layer will consist of a 4×8 APD matrix and 32 LSO crystals ($2 \times 2 \times 6 \text{mm}^3$ front, $2 \times 2 \times 8 \text{mm}^3$ back), yielding a “front layer/back layer” information [17] (see figure 3).

Integrated, 16-channel preamplifiers [18] and 4-channel integrated constant fraction discriminators have been developed. The special electronic boards for the dual layer modules, the compact LSO-APD module with reflector are shown in figure 4.

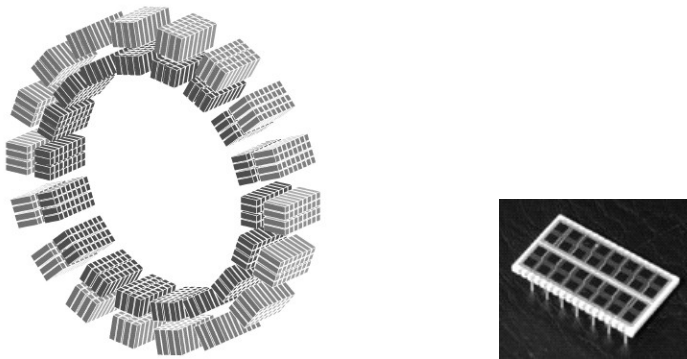


Fig. 3: Left: Position of the LSO crystals in the dual layer LSO-APD tomograph MADPET-II (inner diameter 71 mm). The crystals are optically separated and individually read out by APDs. Right: APD array with 4x8 elements, each element has a sensitive area of $1.6 \times 1.6 \text{ mm}^2$ (Hamamatsu Photonics, Japan).

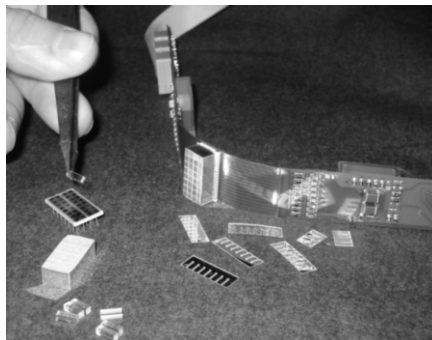


Fig. 4: Mounting of the MADPET-II detector modules. The LSO crystals are individually wrapped in high reflectance foil and glued on the APD array. The modules are connected to the preamplifier chips via flexible boards. This allows to build two radial layers with minimum dead space in between.

Data acquisition in the complete system is based on singles list mode data from all 1152 channels. Coincidence events are sorted by software after the acquisition. This offers maximum flexibility in energy and timing windows. Since the reconstructed field-of-view should cover a large fraction of the detector diameter, a dedicated reconstruction algorithm has been developed which uses the system response matrix from Monte Carlo simulations of the complete system [19-21].

Monte Carlo simulations showed that with this configuration, the reconstructed spatial resolution will be around 1.2 mm and homogeneous throughout the field-of-view of more than 90% of the detector diameter [21, 22].

5. SUMMARY

Positron emission tomography is a functional imaging modality with many clinical as well as research applications. Activity distributions can be reconstructed quantitatively with very high sensitivity. New developments focus on luminous, fast scintillation detectors, compact light sensors and reconstruction algorithms taking into account the precise system response model. Multimodality instruments use the combination of functional (PET) and anatomical information (CT) in one device.

6. REFERENCES

1. Valk, P.E., et al., eds. *Positron Emission Tomography. Basic Science and Clinical Practice*. 2003, Springer: Heidelberg.
2. Defrise, M., A. Geissbuhler, and D.W. Townsend, *A performance study of 3D reconstruction algorithms for positron emission tomography*. *Phys Med Biol*, 1994. 39: p. 305-320.
3. Hudson, H.M. and R.S. Larkin, *Accelerated image reconstruction using ordered subsets of projection data*. *IEEE Trans Med Imag*, 1994. 13: p. 601-609.
4. Fessler, J.A., *Penalized weighted least squares image reconstruction for positron emission tomography*. *IEEE Trans Med Imag*, 1994. 13: p. 290-300.
5. Casey, M.E. and R. Nutt, *Multicrystal two dimensional BGO detector system for positron emission tomography*. *IEEE Trans Nucl Sci*, 1986. 33: p. 460-463.
6. Muehllehner, G., J.S. Karp, and S. Surti, *Design considerations for PET scanners*. *Q J Nucl Med*, 2002. 46(1): p. 16-23.
7. Surti, S., et al., *Optimizing the performance of a PET detector using discrete GSO crystals on a continuous lightguide*. *IEEE Trans Nucl Sci*, 2000. 47: p. 1030-1036.
8. Brix, G., et al., *Performance evaluation of a whole-body PET scanner using the NEMA protocol*. *J Nucl Med*, 1997. 38(10): p. 1614-23.
9. DeGrado, T.R., et al., *Performance characteristics of a whole-body PET scanner*. *J Nucl Med*, 1994. 35: p. 1398-1406.
10. Surti, S. and J.S. Karp, *Imaging characteristics of a 3-dimensional GSO whole-body PET camera*. *J Nucl Med*, 2004. 45(6): p. 1040-9.
11. Watson, C.C., et al., *NEMA NU 2 performance tests for scanners with intrinsic radioactivity*. *J Nucl Med*, 2004. 45(5): p. 822-6.
12. Beyer, T., et al., *A combined PET/CT scanner for clinical oncology*. *J Nucl Med*, 2000. 41: p. 1369-1379.
13. Erdi, Y.E., et al., *PET performance measurements for an LSO-based combined PET/CT scanner using the National Electrical Manufacturers Association NU 2-2001 standard*. *J Nucl Med*, 2004. 45(5): p. 813-21.
14. Surti, S., J.S. Karp, and G. Muehllehner, *Image quality assessment of LaBr3-based whole-body 3D PET scanners: a Monte Carlo evaluation*. *Phys Med Biol*, 2004. 49(19): p. 4593-610.

15. Chatziioannou, A.F., *PET scanners dedicated to molecular imaging of small animal models*. Mol Imaging Biol, 2002. 4(1): p. 47-63.
16. Ziegler, S.I., et al., *A prototype high resolution animal positron tomograph with avalanche photodiode arrays and LSO crystals*. Eur J Nucl Med, 2001. 28(2): p. 136-143.
17. Pichler, B.J., et al., *A 4x8 APD array, consisting of two monolithic silicon wafers, coupled to a 32-channel LSO matrix for high-resolution PET*. IEEE Trans Nucl Sci, 2001. 48: p. 1391-1396.
18. Pichler, B.J., et al., *Integrated low noise, low power, fast charge-sensitive pre-amplifier for avalanche photodiodes in JFET-CMOS-technology*. IEEE Trans Nucl Sci, 2001. 48: p. 2370- 2374.
19. Böning, G., et al., *Implementation of Monte Carlo coincident aperture functions in image generation of a high resolution animal positron tomograph*. IEEE Trans Nucl Sci, 2001. 48: p. 805-810.
20. Rafecas, M., et al., *Effect of noise in the probability matrix used for statistical reconstruction of PET data*. IEEE Trans Nucl Sci, 2004. 51: p. 149-156.
21. Rafecas, M., et al., *Use of Monte-Carlo based probability matrix for 3D iterative reconstruction of MADPET-II data*. IEEE Trans Nucl Sci, 2004: p. 2597-2605.
22. Rafecas, M., et al., *A Monte Carlo study of high resolution PET with granulated dual layer detectors*. IEEE Trans Nucl Sci, 2001. 48: p. 1490-1495.